

Full-round numerical analysis of traditional steel bar and macro synthetic fibre reinforced concrete segments for the Shanghai Metro Extension

Author: Károly Péter JUHÁSZ, JKP Static Ltd., Hungary, office@jkg.hu
Co-author: Lóránt NAGY, JKP Static Ltd., Hungary, lorant.nagy@jkg.hu
Ralf WINTERBERG, EPC Holdings Pte Ltd, rwinterberg@elastoplastic.com

Planning and Designing Tunnels and Underground Structures

Keywords: *fiber reinforced concrete, macro synthetic fiber, full-round modelling, FEA*

1. Introduction

The fibre reinforced concrete (FRC) in question is a short fibre composite, where the matrix is a quasi-brittle material: concrete, and the fibres are made of different materials (e.g. steel, polypropylene, etc.) with different shapes (e.g. round, oval, etc.), random but uniformly distributed, relatively short fibres. The synthetic fibers started to spread in the industry in the last decades, first as micro fibre to prevent early age shrinkage crack of the concrete, than macro synthetic fibres for structural use. These macro synthetic fibres were first used in shotcrete in mines and civil tunnels [2] then slowly introduced to the precast concrete industry (e.g. water tanks), infrastructure (e.g. tramline, road) and the tunnelling industry as primary reinforcing for tunnel segments [10,12]. Today, macro synthetic fibre has a wide range of references in every field of the construction industry.

To reduce or entirely replace steel rebars in a concrete elements with steel fibre already has significant history but with synthetic fibre this is still rather revolutionary. In 2013 the author designed the first synthetic fibre only reinforced concrete grandstand in a sporting stadium in Debrecen, Hungary. This was done without shear links, using only prestressed strands [8]. The system was verified in a real scale laboratory test and compared with the original steel stirrups design. The results exceeded all expectations. The structure had the same capacity as the one with steel shear stirrups and exhibited the same ductile behaviour.

In framing the development of this technology, a further experiment was conducted with a 28 m long beam using the same solution, without steel stirrups. Within these investigations macro synthetic fibres were compared to steel fibres. The results showed that the two materials had the same capacity and same ductile behaviour at given fibre dosages [9]. As well as improving ductility, macro synthetic fibres have been shown to have a number of other advantages compared to all types of steel reinforcement including resistance to corrosion, safe and light to handle and improved economy [2].

Today we can design and verify all material properties and any scenario where the beneficial influence of macro synthetic fibres might be significant, by means of FEA solutions. The author has focused on a new kind of FEA with an advanced fibre reinforced concrete (FRC) material model, utilising the software suite Atena (Cervenka Consulting). The new FRC material model, called Modified Fracture Energy [5], provides a relatively simple way to model FRC.

The work referred to in this paper relates to a typical TBM tunnel in Shanghai's Metro extension, the object being to optimize the reinforcing solutions using macro synthetic fibres. In this paper, the authors are presenting their solutions in comparison to the physical real scale tests, which were carried out at Tongji University in Shanghai by Professor Lui, X [1].

2. Original design and laboratory test

2.1 Geometry and reinforcement

This typical Shanghai metro tunnel example has an inner diameter of 5500mm, an outer diameter of 6200mm and a wall thickness of 350mm. One ring is made from six segments. The key and the invert segment have a different geometry and reinforcement whilst the lateral ones are identical. The invert segment has an angle of 84 degrees, the key 16 degrees, and the four sides 65 degrees. The longitudinal length of one segment is 1200mm. The segments were connected with 400 mm long and 30 mm diameter straight bolts at two points, so the six segments were connected at 12 points. The longitudinal bolts are similar to the circumferential. Only one ring was checked in the laboratory test so the longitudinal connections were not included in the test. The segments were hoisted at two points whereas the key segment was hoisted at a single point only. Geometry and loading configuration can be seen in Figures 1 and 2.

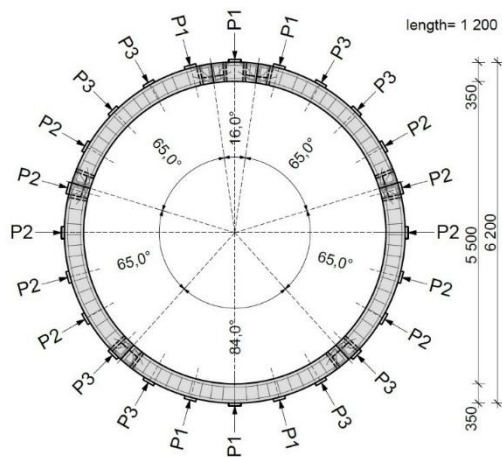


Fig. 1: Geometry and loading configuration of the tunnel

Fig. 2: One to one laboratory test of the tunnel

The aspect ratio of the segments, which is the developed length over the lining thickness, computes to 12.2 for the invert segment and 9.5 for the regular lateral ones. Given that a segment aspect ratio not exceeding 10 generally provides a safe opportunity for a fibre only solution, the lateral segments present no problem [14]. However, the invert segment's aspect ratio is over this threshold, so it was decided to use combined steel bar and synthetic fibre reinforcement for the numerical studies.

The steel reinforcement, as per the original design, altogether amounts to a total of 559kg per ring. This yields an average reinforcement ratio of 72kg per cubic meter of concrete for the invert and side segments. This is not a very high degree of reinforcement, however, the other driver in using FRC for segmental linings is the enormous gain in productivity, giving this technology more and more momentum in countries with already high or still soaring labour costs, such as China. Replacing the complex rebar cages of a segment cuts out the time required for cutting and bending, fixing or welding, placing and checking of the position of the cage. Entire replacement by fibres can reduce the segment production cycle time down to 50%, such as in the case of the Hobson Bay project in Auckland, New Zealand, which in return leads to substantial cost savings [13].

2.2 Materials

The general tests to characterize the materials were carried out after the full scale laboratory test. The mean concrete compressive strength was determined to be 50MPa cubic, the strain at this stress was 1.8‰ (0.0018). A concrete class C40/50 according to the European design standard was used, Eurocode 2, for the finite element analysis. The grade of the steel bar reinforcement was HRB335 with a yield strength of 335 MPa, using ribbed bars.

2.3 Full scale laboratory test

Tongji University in Shanghai has carried out a full scale test in their laboratory loading a full segmental ring and measuring the load and the referring displacements. The ring was loaded at 24 points, with hydraulic jacks located every 15 degrees. The load was distributed on the ring by means of transverse beams onto the segments as a line load. This closely spaced, distributed load modelled the loading from the soil under permanent condition. The load configuration and the one to one laboratory test setup can be seen in Fig. 1 and 2.

During loading the 24 loading jacks applied varying levels of load. At the invert and at the crown a load P_1 was acting at three points respectively. At the benches the load P_2 was applied as a function of P_1 and at the walls a load P_3 as a function of P_1 and P_2 . Because of the different loads the structure not only experienced different central thrust force, but has undergone eccentricity as well, modelling the real conditions of the tunnel.

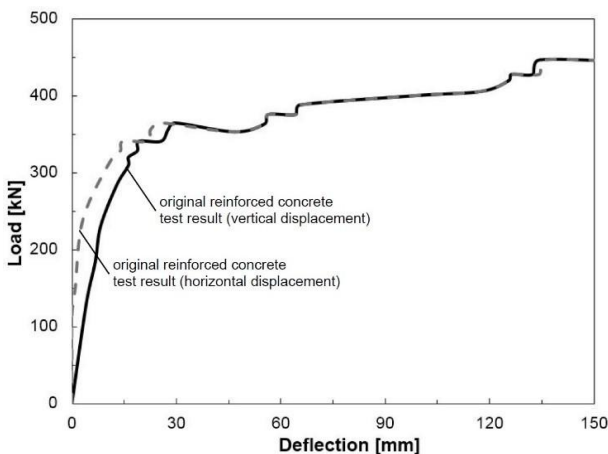
The loading phase had two stages. In the first stage the functions of the loads were the following:

$$P_2 = 0.65P_1 \text{ and } P_3 = (P_1 + P_2)/2 = 0.825P_1$$

Load P_1 was increased until P_2 reached its design value which was 292.5kN.

In the second stage the load P_2 was unchanged, where load P_3 had the following function:

$$P_3 = (P_1 + P_2)/2$$



angles, which can be seen in Fig. 3.

and P_1 was increased until its design value of 455kN. With these functions it was able to model the loading changes as a function of the tunnel depth below surface.

The displacement was measured at 14 points of the ring at the following angles: 0, 9, 40, 74, 90, 105, 139, 180, 223, 255, 270, 288, 320 and 353 degrees. The most important positions herein were the 0, 180, and the 90, 270 degrees positions, which are measuring the horizontal and vertical displacements. From these results a load-displacement diagram was generated, showing load P_1 over the displacements at the different

Fig. 3: Load-deflection diagram result of the one to one laboratory test

3. Finite Element Analysis of the tunnel

3.1 Material tests for input of the FEA

The common test for fibre reinforcement concrete is the standard 3 or 4 points beam test. In our case 4 point beam tests was carried out with plain concrete and different dosages of macro synthetic fibres, using the original concrete mix designs. The test was made at Tongji University, with the help of Dr Stefan Bernard (TSE) and Andrew Ridout (EPC). Although, there is no method to evaluate the material parameter from round panel test this is one of the most widely used material test in the tunnel industry. Because of this in addition round determinate panel (RDP) (ACI C1550) tests were also conducted.

Four point beam tests were carried out using 150mm x 150mm section beams, 550mm long. The beam was supported on 450mm span and the load was applied in the third points. The beam was loaded until 4mm central displacement and the load-displacement diagram was recorded. This generated information about the behaviour of the fibre reinforced concrete, such as flexural strength, post crack strength and ductility. To measure and compare the ductility of the different beam test results the area under the load-displacement diagram was measured, and called as

work of fibre: W_f . Other way is to calculate the R_{e3} number according to Japanese standard (JSCE SF-4, 1985) [6], which is the ratio of average post-crack residual load and peak (first crack) load in percentage terms.

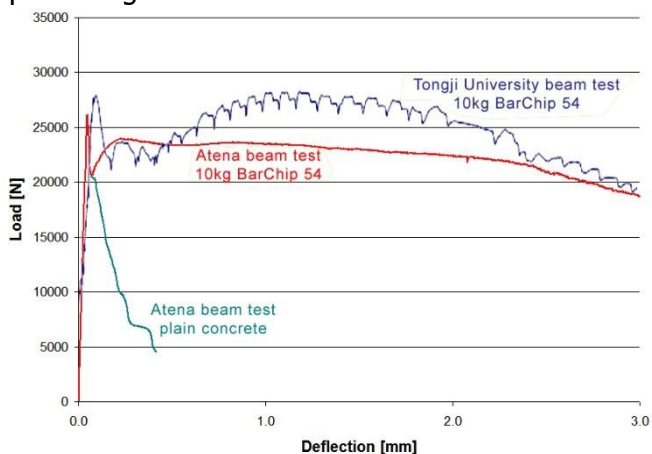


Fig. 4: Beam test result and numerical modelling

This method contains an inaccuracy as the peak load has a relatively big dispersion, moreover the fibre reinforcing has no effect on the peak load. The material tests for FRC were done with 6 and 10kg/m³ dosage of macro synthetic fibre. The resultant W_f/R_{e3} numbers were 50J/54.6 and 75J/81.6 respectively. Figure 4 shows the test results and the numerical modelling of the beam test.

3.2 Material model of concrete and FRC

Concrete is a difficult material to model. First of all it exhibits different behaviour in compression and in tension: on the compression side it exhibits a strain hardening behaviour with a relatively high (~10 times larger) compressive strength than tensile strength, while on the tension side it exhibits a quasi-brittle material behaviour. Furthermore, the concrete exhibits creep in response to persistent loading, and because of brittle behaviour does not respond well to dynamic effects. For this reason the concrete is designed with high safety factors (generally concrete material safety factor according to EC is $\gamma_c=1.50$ while steel has $\gamma_s=1.15$).

To model concrete adequately the material model will need to combine different behaviours in compression and tension, this is called 'combined failure surfaces'. There are many such models available in the literature, the most commonly used are: Von-Mises and Rankine; Drucker-Prager and Rankine; and Mentérey-William and Rankine (Rankine cube is at the tension side). However, it is important to note that these models only define the peak strength of the material, not the post-cracking response. Numerous other models can be used to approximate the post-cracking capacity of FRC.

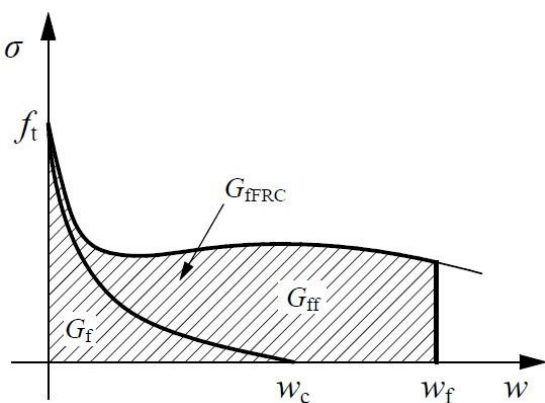


Fig. 5: Fracture energy diagram

When stresses exceed the tensile strength of the concrete it will crack. There will be a residual stress at the crack surface that depends on the crack width opening distance. This stress is associated with an energy, called fracture energy (G_f). This energy is influenced by the aggregate type (round or crushed), size, and its bond to cement mortar. Fibres increase this fracture energy (G_{fFRC}), thereby making the concrete a more ductile material. This approach called modified fracture energy method [5]. The most important criterion for the selection of the FRC material model is to be able to model this increased fracture energy (G_{fFRC}) and select a value that is appropriate to the FRC used for a design (eg. Fig. 5).

Here the difference between steel and macro synthetic fibre reinforced concrete needs to be discussed. Generally the result of a load-CMOD or load-deflection diagram for a normal dosage of steel fibres (~30-50 kg/m³) and a normal dosage of macro synthetic fibres (~5-8 kg/m³) are roughly the same. Steel fibres generally offer high resistance at smaller crack openings, but macro synthetics work better across wider cracks (Fig. 6). These generalisations depend on the dosage rate of the fibres selected.

The stress-crack width relation required in a FEA must be determined by an inverse analysis of beam test results. The inverse analysis was carried out by means of a virtual beam test, which is modelling the real beam in the finite element software, yielding the same load and deflection that occurred in physical tests. The inverse analysis iterations were made until the W_f/R_{e3} numbers matched those in the physical material tests. The W_f/R_{e3} values were 50J/56.7 at 6kg/m³ and 75J/85.1 at 10kg/m³ of dosage, respectively. The inverse analysis showed good correlations with

the real beam test results, see Figure 4. To model the added fracture energy we use a tension stiffening effect on the tensile surfaces of the concrete elements, where the post-crack performance contributed by the fibres defines the added fracture energy (Fig. 6). The stress-crack width diagram was limited to 3mm crack width opening, as a limit from an engineering point of view. However it never reached this value even in the ULS condition.

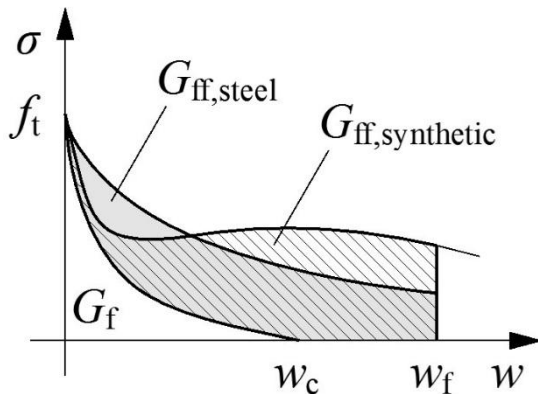


Fig. 6: Differences between fracture energy of steel and synthetic fibre reinforced concrete

The concrete was modelled as a three dimensional (3D) brick element with a material model consisting of a combined fracture-plastic failure surface [3]. Tension is handled herein by a fracture model, based on the classical orthotropic smeared crack formulation and the crack band approach. It employs the Rankine cube failure criterion, and it can be used as a rotated or a fixed crack model. The plasticity model for concrete in compression uses the William-Menétrey failure surface [11]. Changing aggregate interlock is taken into account by a reduction of the shear modulus with growing strain, along the crack plane, according to the law derived by Kolmar [7].

The concrete has a stress-strain diagram according to Eurocode 2 [4]. The crack width was calculated from the stress-crack width diagram, determined by means of inverse analysis, with the help of the characteristic length, which is a function of the size of the element and the angle of the crack within the element. This method is the only one that could realistically represent the cracks in the quasi-brittle material. This is the main advantage of this advanced material model.

3.3 Other materials for FEA

Steel rebars and bolts were modelled as discrete link elements with a uniaxial ideal elastic-plastic stress-strain material model. The rebars link element was connected to every single concrete brick element which was crossed. The bolts had no connection with the concrete brick elements, however, at both ends they were held by the nuts on the concrete surface, which were only able to undergo tension.

The connection surface of two adjacent segments was connected with an interface material, which could hold compression only through friction on the surface. With this special interface material the connections of the segments were modelled, which could be open or closed for bending, where tension would be held by the connection bolts.

3.4 Numerical model of the tunnel

After defining the accurate material model the geometry was defined. Firstly, the concrete and reinforcement and then the loads and supports must be defined. The tunnel is symmetric at the horizontal and the vertical axis, so only a quarter of the full ring geometry is sufficient to model the structure with symmetrical support conditions on the symmetrical plane. This also helps to define the boundary conditions and makes the calculation faster. Finally, the monitoring points need to be defined, where the load and resulting displacements were to be measured. The loads were positioned at exactly the same locations and with the same values as in the full scale laboratory test.

3.5 Calculation of the FEA

The FEA was solved with the Newton-Raphson method. The lack of this method, being unable to handle load drops after crack localisation, was overcome by the fact that explicit load drops did not occur during the trials (Fig. 3). The calculation took 4.88 Gigabyte memory and solved millions of equations in approximately 1000 steps, taking 12 hours until the results were available. The full model comprised 6300 elements, although only a quarter of the ring was taken into account.

4. Results of the Finite Element Analysis

4.1 Result of the original RC solution

After running the FEA the results were checked. Most important was the load-displacement diagram, which was compared to the full scale laboratory result. It can be seen in Fig. 7 that the result of the laboratory test and the result of the FEA are similar in both characteristic and values and show the same maximum load capacity.

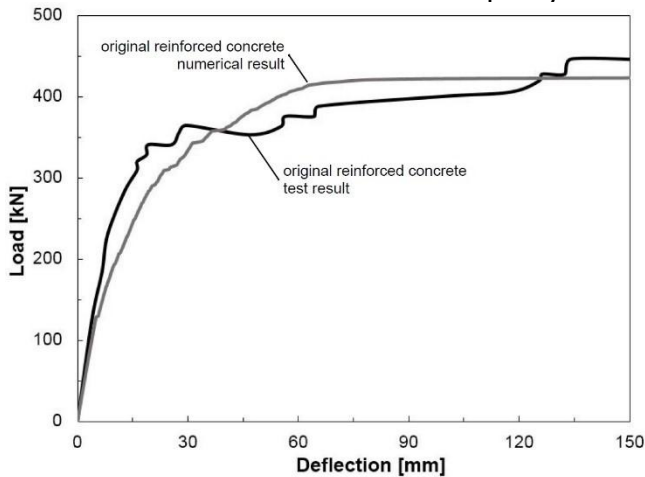


Fig. 7 Load-deflection diagram result of the original RC solution

The maximum compressive stress of the concrete was 35.9 MPa, while the maximum crack width just before complete failure was 5.0mm. The steel bars were grouped according to the stress-levels experienced and selection was based on the ones that could be said to be not providing any input and which could be reduced or completely omitted as a first step. According to the computed stress levels, the remaining steel bars could be reduced in diameter in accordance with the computed stress value. Full animation could be done and the entire loading process could be observed from the formation of the crack until total failure. In this way the weak points of the tunnel and the type of failure could be visualised easily. For this type of tunnel and its loading, the mechanism of failure was at the

segment joints where the connecting bolts burst out from the concrete, see Figure 10.

4.2 Optimizing the segmental lining with synthetic fibre reinforcement

After the successful modelling of the original RC ring, the optimization could be started, re-calculating with reduced steel bars and added fibre. Firstly, the lowest stress-level steel bars were omitted and replaced with a moderate dosage of fibre. Then, with increasing fibre dosage, more and more steel bars were omitted. These calculation processes were laborious as adding fibre also changes the occurring deformations, thereby changing the arising eccentricity, and eventually, can change the failure mode, too. However, the ruling failure mode always was radial joint bursting at the bolt pockets.

4.3 Optimized results

After these calculations were made three viable solutions were proposed, which can be taken from Table 1.

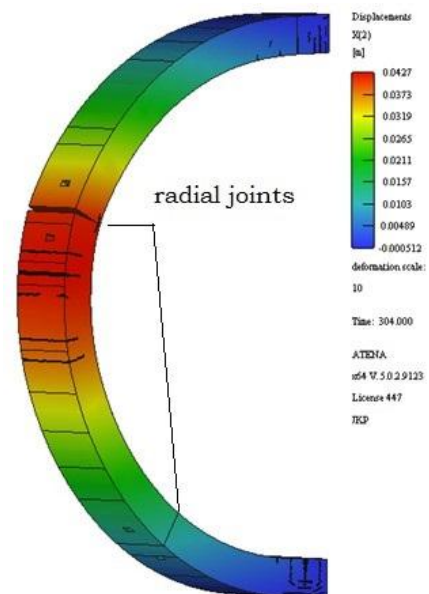


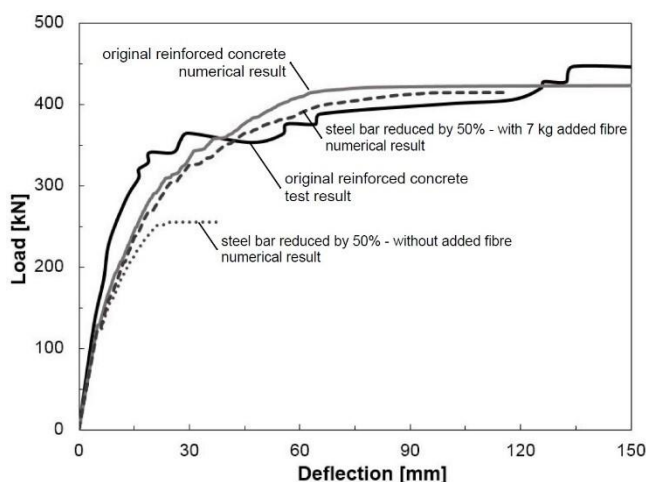
Fig. 8: Horizontal displacement and crack configuration at failure (ULS)

Table 1: Optimized solutions of the tunnel

	original solution	solution 1	solution 2	solution 3
added fibre (kg/m ³)	-	6	7	10
max. crack width (mm)	5.0	2.3	2.1	1.9
bottom segment (kg)	134.7	88.1	61.3	22
side segment (kg)	95.9	56.1	49.5	28.6

key segment (kg)	40.7	31.8	23.1	17.1
total tunnel	559kg steel	344.3kg steel (-39.8%) +46.3kg fibre	282.4kg steel (-49.5%) +54.0kg fibre	140.4kg steel (-75.0%) +77.2kg fibre

Adding fibre in conjunction with steel bar reduction improved control of both crack width and crack propagation. The crack width of the original RC solution was 5.0mm before total failure, where in solution one this was reduced to only 2.3 mm with less visible cracks. This is a reduction of crack widths of more than 50%, which provides a substantial gain of durability. The results of the calculations with optimized reinforcement can be seen in Fig 9.



From the calculated solutions, number two seemed to be the most viable. However, the FEA is valid only for this given situation, where for other conditions more parameters would need to be checked. The characteristic failure mode occurred at the radial joints (connection bolts and their surrounding area) so review and redesigning of this part could lead to a more optimized solution. The final recommendation is 7kg/m³ macro synthetic

fibre in conjunction with 50% steel rebar reduction. This solution is planned to be verified by physical laboratory testing in the near future.

Fig. 9: Load-deflection diagram result of optimized solutions

5. Conclusions

A full scale TBM segmental tunnel ring was modelled with an advanced material model in FEA. By using the modified fracture energy method an accurate material model can be used for FRC. A typical Shanghai Metro extension TBM tunnel segmental ring was tested to full scale at the Tongji University, Shanghai, and the load-displacements results were compared with the FEA. The similarity was deemed appropriate, so the model has been justified. Low-stressed steel bars within the section were reduced and macro synthetic fibre was added to the structure. By using macro synthetic fibre reinforcement the volume of steel bars could be reduced. This, in return, leads to significant cost savings in both material and labour, as well as a reduction of the production cycle times.

6. Acknowledgements

The authors would like to thank Professor Bai Yun (Tongji University, Shanghai, China) for his help and support during the modelling.

7. References

- [1] Bi X, Liu X and Wang X, in press. Experimental investigation on the ultimate bearing capacity of continuous-jointed segmental tunnel linings, China Civil Engineering Journal.
- [2] Bernard E S, Clements M J K, Duffield S B, and Morgan D R, 2014. Development of Macro-Synthetic Reinforced Shotcrete in Australia, 7th International Symposium on Sprayed Concrete, Norway, June 2014.
- [3] Cervenka J and Papanikolaou V K, 2008. Three dimensional combined fracture-plastic material model for concrete, in International Journal of Plasticity (24): 2192-2220.

- [4] EUROCODE EN 1992, 2004. European Code for design of concrete structures, European Committee for Standardization (CEN). Available from: <http://eurocodes.jrc.ec.europa.eu/> (European Committee for Standardization)
- [5] Juhasz K P, 2013. Modified fracture energy method for fibre reinforced concrete, in *Fibre Concrete 2013: Technology, Design, Application* (ed. Kohoutkova A, et al) pp 89-90 (Faculty of Civil Engineering Department of Concrete and Masonry Structures: Prague)
- [6] JSCE SF-4, 1985. Japanese code for test for flexural strength and flexural toughness of SFRC. Available from: <http://www.jsce-int.org/> (Japan Society of Civil Engineers)
- [7] Kolmar, W, 1986. Beschreibung der Kraftuebertragung über Risse in nichtlinearen Finite-Element-Berechnungen von Stahlbetontragwerken, Dissertation, T.H. Darmstadt.
- [8] Kovacs, G and Juhasz, K P, 2013. Precast, prestressed grandstand of PFRC in stadium, Hungary, in *Central European Congress on Concrete Engineering: Concrete Structures in Urban Areas* (ed. Biliszczyk J, Bien J, Hawryszkow P and Kaminski T) Paper 104 (CCC Central European Congress on Concrete Engineering: Wroclaw)
- [9] Kovacs, G and Juhasz, K P, in press. Synthetic and steel fibres in prestressed, precast long span beams, 10th CCC Congress LIBEREC 2014
- [10] Martin, G, 2012. The case for structural synthetic fibres, in *Tunnels and Tunneling*, May 2012: 38-40
- [11] Menétrey P and William K J, 1995. Triaxial Failure Criterion for Concrete and Its Generalization, in *ACI Structural Journal*, 92(3): 311-318.
- [12] Ridout, A, 2008. Macro-synthetic fibre for segmental linings and other precast concrete elements, in *Concrete*, September 2008: 41-42
- [13] Winterberg, R and Vollmann, G, 2009. Einsatz von Stahlfaserbeton in der Tübbingproduktion: Bauverfahren und Kriterien zum Einsatz von Stahlfaserbeton, Fallstudie Hobson Bay Tunnel / Use of steel fiber reinforced concrete in precast tunnel segment production: Construction methods and criteria for the use of steel fiber reinforced concrete, case study Hobson Bay tunnel; BFT Betonwerk + Fertigteiltechnik Heft 04/2009, Bauverlag, Gütersloh, April 2009
- [14] Winterberg, R, 2012. Segmental Tunnel Linings with Fibre Reinforced Concrete, *SPET Journal* No. 35, Society of Professional Engineers Thailand, Bangkok, June 2012